Chapter 12

Electrolysis for Ozone Water Production

Fumio Okada and Kazunari Naya

Additional information is available at the end of the chapter

http://dx.doi.org/10.5772/51945

1. Introduction

OH radicals produced by ozone decomposition in water are the second strongest oxidizers after fluorine. Therefore, ozone water is used in a wide range of applications, such as the sterilization of medical instruments, the oxidation and detoxification of wastewater, the deodorization and decoloration of well water, the cleaning of electronic components, and food treatment [1, 2]. For example, the possible applications of ozone water to the control of microbiological safety and the preservation of food quality are well summarized in a review paper [3]. · OH radicals can also kill various bacteria, such as O157, MRSA, *Pseudomonas aeruginosa*, *Bacillus subtilis*, *Bacillus anthracis*, *Bacillus cereus* and *Legionella pneumophila* [4].

There are two major processes for ozone water production as shown in Fig. 1. One is a gas phase ozone production followed by mixing ozone with water [Fig. 1(a)]. In this process ozone gas is produced from oxygen gas using electric discharge, and then mixed with water using hollow fibers or mechanical mixers. Although this process can supply ozone water at a low electric cost, it requires a high-voltage power supply, an oxygen cylinder, and a mixing process. Therefore, the system is large and cumbersome in operation, and the facility cost is high. The other process is direct water electrolysis using a polymer electrolyte membrane (PEM) [Fig. 1(b)]. In this process, water is introduced to the anode side of the electrolysis cell, electrolytically decomposed, converted to ozone, and mixed with the ozone gas formed in the compact cell. Such apparatuses can enable ubiquitous and low-voltage operation as home electronics.

The ozone formation reactions and standard electrode potentials in the direct water electrolysis are as follows:

Anode:

$$2H_2O \rightarrow O_2 + 4H^+ + 4e^- \quad E^0 = 1.229\ V \tag{1}$$

$$3H_2O \rightarrow O_3 + 6H^+ + 6e^- \quad E^0 = 1.511\ V \tag{2}$$

$$O_2 + H_2O \rightarrow O_3 + 2H^+ + 2e^- \qquad E^0 = 2.075\ V \tag{3}$$

Cathode:

$$2H^+ + 2e^- \rightarrow H_2 \qquad E^0 = 0\ V. \tag{4}$$

These reactions are fundamental in electrochemistry and have been extensively studied. Ozone gas evolves by a six-electron reaction in Eq. (2) at a voltage higher than 1.511 V, accompanied by oxygen evolution. By increasing voltage to above 2.075 V, the oxidation of O_2 gas to form O_3 is also expected as shown in Eq. (3). Since O_2 evolution occurs at lower potential than O_3 evolution, the production rate and electric power consumption in O_2 evolution are much higher than those in O_3 evolution. Therefore, catalytic activity in O_3 evolution reactions is indispensable for electrolysis cell design.

Current efficiency or charge yield, $\Phi^e_{O_3}$ (%), and power efficiency or specific energy consumption, $w^e_{O_3}$ (kWh/kg-O_3), were calculated using

$$\Phi^e_{O_3} = \frac{5 \times F \times Q}{3 \times M_{O_3} \times I} \times 100\ (\%), \tag{5}$$

$$w^e_{O_3} = \frac{I \times U}{1000 \times Q}\ (\text{kWh/kg-}O_3)\ , \tag{6}$$

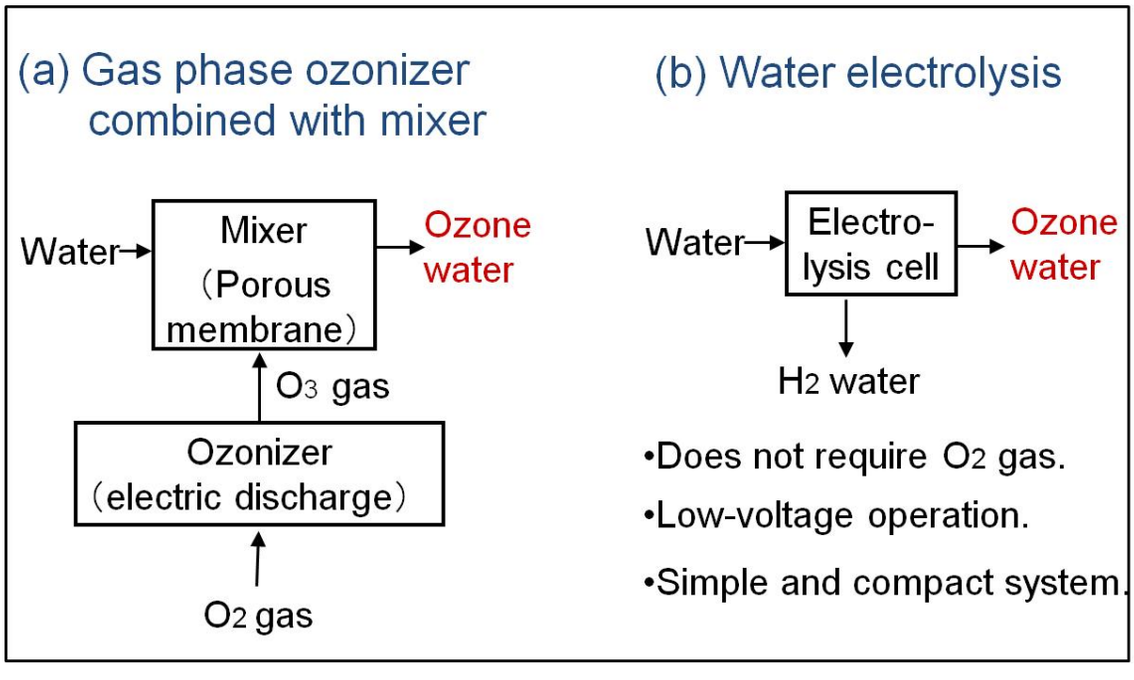

Figure 1. Two types of representative ozone water production systems.

where F is Faraday's constant (9.6485 x 10^4 C/mol), Q is the O_3 production rate (kg/h), M_{O_3} is the molecular weight of O_3 (48), I is the current (A), and U is the potential difference between the anode and the cathode (V). The derivation of Eq. (5) is as follows:

When the current I (A) is applied to the cell, the electron flow rate per hour is written as

$$\frac{I}{F}\times 3600\left(\mathrm{mol/h}\right). \tag{7}$$

O_3 produced per hour, Q (kg/h), can be converted to mol/h using

$$\frac{Q}{M_{O_3}}\times 10^3\left(\mathrm{mol/h}\right). \tag{8}$$

Because six electrons are required to produce one O_3 molecule, 1/6 of the electron flow rate calculated using Eq. (7) becomes the theoretical and maximum O_3 molecule production rate, which corresponds to 100 % efficiency. Therefore, real current efficiency is defined by

$$\Phi^{e}_{O_3}=\frac{\frac{Q}{M_{O_3}}\times 10^3}{\frac{I}{F}\times 3600\times\frac{1}{6}}\times 100\,(\%). \tag{9}$$

Calculating the right-hand side of the equation above, we obtain

$$\Phi^{e}_{O_3}=\frac{5\times F\times Q}{3\times M_{O_3}\times I}\times 100\,(\%).$$

The electrochemically produced O_3 molecules decompose in anode water to form OH radicals. The decomposition reaction is very complicated, and more than 30 elemental reactions are involved in the process. The reaction set proposed by Wittmann, Horvath and Dombi (WHD model) consists of 33 elemental reactions [5]. Although many reactions are taken into consideration, the decomposition behavior of O_3 in neutral pH water cannot be reproduced adequately using the WHD model.

The actual half-life of O_3, *i.e.*, about 2 h in ion-exchanged water and 4 h in pure water, are much longer than the calculated values. To improve the accuracy of the elemental reaction set, Mizuno *et al.* proposed new rate constants in a few elementary reactions [6]. They reduced the rate constants in OH^- formation reactions up to three orders of magnitude to fit their experimental data. We also noticed a discrepancy between the actual and estimated half-lifes, and obtained findings similar to those by Mizuno et al. However, we were not as radical as them. We would not write a paper, because we did not obtain experimental evidence to confirm the small rate constants of OH^- formation reactions.

For readers of this chapter, a simplified image of the·OH radical formation reactions is presented below:

$$O_3 + OH^- \rightarrow HO_2^- + O_2 \quad (10)$$

$$O_3 + HO_2^- \rightarrow O_3^- + HO_2 \quad (11)$$

$$O_3^- + H_2O \rightarrow \cdot OH + O_2 + OH^- \quad (12)$$

Sum of Eqs. (10) to (12):

$$2\,O_3 + H_2O \rightarrow \cdot OH + 2\,O_2 + HO_2 \quad (13)$$

O_3 decomposition is started by the reaction of O_3 with OH^-, forming HO_2^- as in Eq. (10). The initiation of O_3 decomposition is pH-dependent, because OH^- concentration determines the reaction rate in Eq. (10). Therefore, water pH strongly affects the half-life of O_3, *i.e.*, O_3 has a shorter half-life in alkaline water and a longer one in acidic water. HO_2^- reacts with another O_3 molecule to form O_3^- [Eq. (11)]. Finally, O_3^- is converted to a · OH radical by reacting with H_2O [Eq. (12)]. Eq. (13), the summation of Eqs. (10) to (12), indicates that one · OH radical is produced from two O_3 molecules, which means that · OH radical formation is a second-order reaction of O_3. Therefore, four times higher · OH radical concentration will be obtained by doubling the O_3 concentration in water. The bactericidal power of ozone water is also the second order of the O_3 concentration in water.

The development of electrochemical ozone production (EOP) systems using a PEM has shown significant progress. The main interest in studies of EOP systems has been in the preparation of effective anodes aiming at high catalytic activities for O_3 evolution. Many anode substances have been tested in a PEM system. The first demonstration of highly concentrated and efficient EOP using a PEM system was reported by Stucki *et al*. [7], who used a PbO_2 layer as an anode catalyst. They obtained a current efficiency of more than 15 %. Since then, studies on ozone water production using PEM systems have become an active area. Feng *et al.* utilized an Fe-doped PbO_2 catalyst electrodeposited on a Ti tube, and obtained a current efficiency of more than 12 % in 0.52 M K_2PO_4/0.22 M KH_2PO_4 buffer containing 2.5 mM KF [8]. Santana *et al.* reported that an IrO_2-Nb_2O_5 catalyst deposited on a Ti anode shows a current efficiency of 18 % in 3 M H_2SO_4 + 0.03 M KPF_4 solution, but its lifetime is only about 1 h: the corrosion of the anode catalyst prevents the system from longer operation [9]. Chang *et al.* utilized an Sb-doped SnO_2 anode catalyst, and obtained a current efficiency of more than 15 % in 0.1 M HCl solution [10]. They improved the efficiency up to 36.3 % in 0.1 M H_2SO_4 solution by changing the anode catalyst to Ni- and Sb-codoped SnO_2 [11]. Awad *et al.* showed a current efficiency of 11.7 % using a TaOx/Pt/Ti anode electrode in tap water, and reported that the system could be operated for as long as 65 h [12]. B-doped diamond substrates have been used as an anode, and Arihara *et al.* reported a stable operation with a current efficiency of 29 % in 1 M H_2SO_4 solution [13]. Recently, Kitsuka *et al.* have reported that a high current efficiency of 9% was achieved at a low current density of 8.9 mA cm^{-2} in 0.01 M $HClO_4$ at 15°C using n-type TiO_2 thin films deposited on Pt/TiO_x/Si/Ti substrates [14].

The generation mechanism of · OH radicals in a B-doped diamond electrode system was investigated by Marselli *et al.* by ESR spectroscopy in the presence of the spin trap 5,5-dimethyl-1-pyrroline-*N*-oxide (DMPO), and the formation of · OH radicals during water electrolysis was confirmed [15].

However, several problems remain unsolved for the commercial applications of the PEM system: Some catalysts, such as PbO_2 and Sb, are harmful to the human body and cannot be used for systems where contact of the human body with ozone water is inevitable; the use of an electrolyte, such as HCl or H_2SO_4, is also undesirable for the same reason; diamond substrates are inferior in forming water flow channels that enable good contact between ozone and water in the apparatus; and no catalyst lifetime longer than 500 h has been reported yet. Therefore, improvements in the performance and stability of the PEM system are still necessary.

Pt electrodes have been a classic substance for water electrolysis, and thus we have reinvestigated the potential of a Pt anode used in a conventional PEM system. There is an encyclopedia of studies of O_2 formation by the electrochemical splitting of water using Pt electrodes [16]. However, research on EOP is a rather limitted. The current efficiencies of Pt electrodes were reported in the above-mentioned studies, because researchers measured the efficiencies of Pt electrodes as references for comparison with those obtained using their original anode catalysts.

The current efficiency range of the Pt anode is from 0.7 to 7 %, and strongly depends on the system setup. If a high efficiency and a long lifetime could be achieved using a Pt electrode, we would eventually obtain a reasonably priced and safe EOP system.

In our research, an EOP system using Pt mesh electrodes combined with a conventional PEM, *i.e.*, Nafion 117 membrane, was investigated in terms of current efficiency and lifetime. We found that Pt particles that dissolve from the Pt anode migrate through the membrane, and are dendritically deposited on the cathode surface in contact with the membrane. The deposited Pt particles decompose the membrane, decreasing the current efficiency and lifetime of the EOP system. As a solution to solve this problem, one of the key improvements is achieved in our EOP system: A quartz felt separator is inserted between the membrane and the cathode. Pt particles are captured and isolated in the separator. Therefore, no decomposition occurs in the membrane [17].

Another important improvement is realized by the appropriate selection of a cathode electrolyte (catholyte). When a NaCl catholyte with concentrations higher than 0.085 M is circulated on the cathode side of the cell, the formation rate of Pt oxide on the anode surface is markedly reduced. Cl^- ions that migrated from the catholyte to the anode surface inhibit PtO_2 formation. The anode surface is kept clean during the EOP operation, and the clean Pt surface provides both good current efficiency and long lifetime [18]. As a result, the new EOP system achieved a high current efficiency of more than 25 % and a lifetime longer than 2,000 h. These findings and experimental results are presented in this chapter.

2. Conventional electrolysis system and its performance

2.1. Structure of conventional electrolysis cell

Photographs of electrolysis cells for the EOP system are shown in Fig. 2. A small-capacity cell that can produce ozone water up to a flow rate of 1 L/min is shown in Fig. 2(a), and a large-capacity cell for 20 L/min ozone water production is shown in Fig. 2(b). Both cells are designed and manufactured by FRD, Inc. The electrolysis cells consist of a Nafion 117 membrane sandwiched by Pt #80 mesh electrodes and have Ti and stainless terminal plates.

The cross-sectional cell configuration and the cathode structure of the small cell are shown in Figs. 3(a) and 3(b), respectively. The #80 Pt mesh electrodes are 4 x 2 cm^2 in area, 0.2 mm in thickness, and 0.3 mm in pitch distance. To form a waterway, a Ti #40 mesh is inserted between the Ti plate and the Pt mesh on the anode side, and a SUS304 #100 mesh is inserted between the SUS304 plate and the Pt mesh on the cathode side. The electrodes are held by SUS304 and Ti plates, which act as the cathode and anode terminals, respectively. The use of the mesh and plate made of Ti is important, since SUS304 cannot withstand oxidative corrosion caused by anode electrolysis reactions.

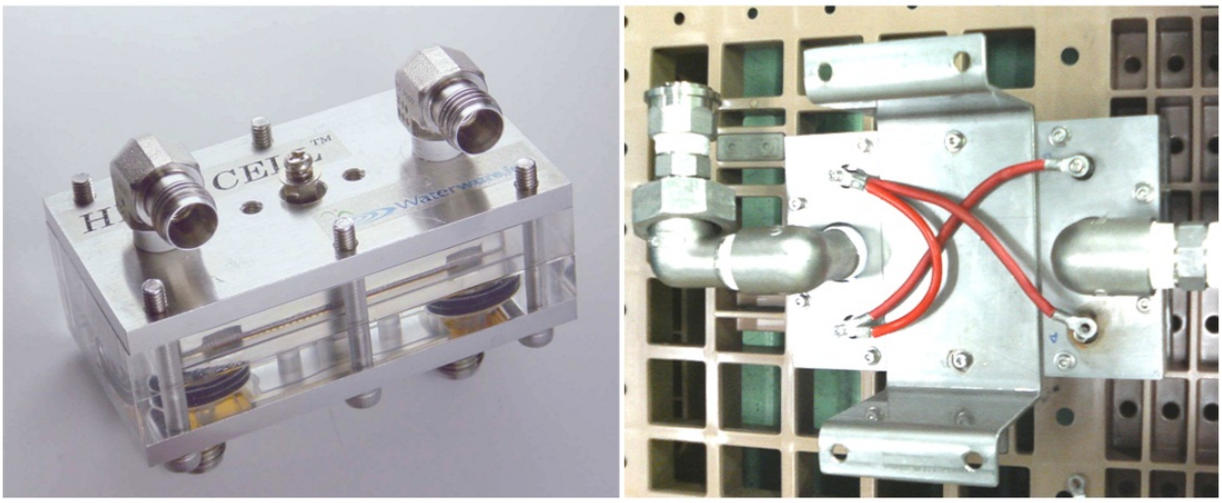

(a) 1 L/min O_3 water production cell (b) 20 L/min O_3 water production cell

Figure 2. O_3 water production cells using Pt electrodes and Nafion membrane. Copyright: FRD, Inc.

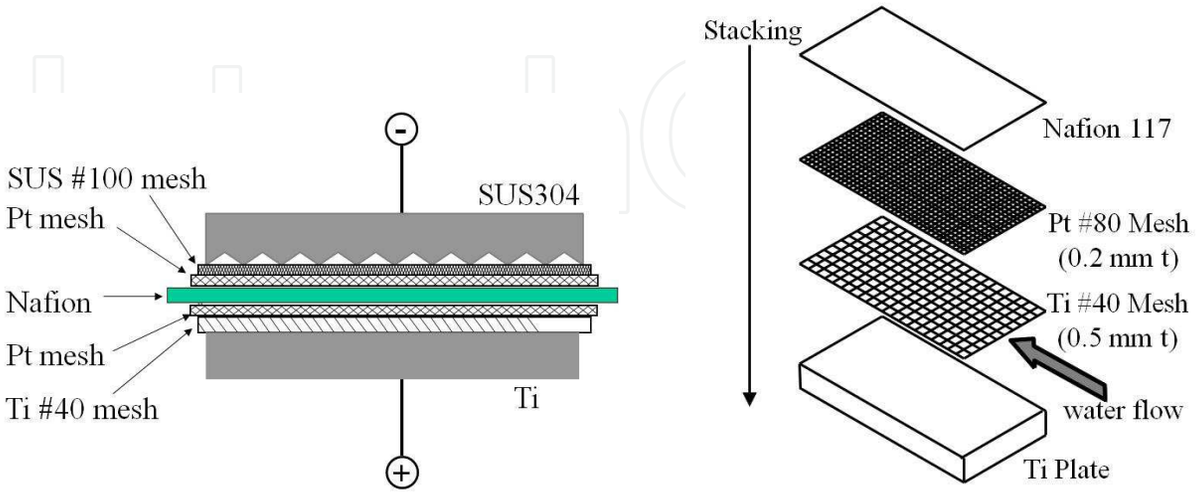

(a) Configuration of 1 L/min cell

(b) Cathode structure of 1 L/min cell

Figure 3. Cross-sectional views of 1 L/min electrolysis cell [17]. Reproduced with permission from The Electrochemical Society.

The flowchart of the EOP system is shown in Fig. 4. Tap water was passed through Na-type ion-exchange resin (Rohm and Haas, Amberlite IR-120B Na) to eliminate Ca^{2+} ions that lead to Ca_2CO_3 deposition on the anode and decrease the efficiency of the system. The ion-exchanged water is introduced into the anode and cathode at flow rates of 300-900 mL/min. Since the solubility and decomposition rate of ozone in water depend on water temperature, the temperature of the supplied water was controlled to 20 ± 1 ºC using a heat exchanger (HB Corporation, TEC1-127B) . However, temperature control is unnecessary for the practical use of the system.

The voltage and current of the electrolysis cell are controlled by a programmable power supply (TDK-Lambda Corporation, ZUP20-40) and monitored by using an A/D converter (Pico Technology, ADC-16). Ozone water and gas phase ozone were sampled in a 1-cm-optical-length cell, and ozone concentration was spectroscopically determined using a compact UV-VIS absorptiometer (Shimazu UV mini-1240). Ozone-containing gas was sampled by replacing water in the optical cell. Although water droplets remained in the cell after the gas sampling, the absorption and scattering caused by the droplets were measured by replacing the captured O_2 and O_3 gas mixture with air, and they were then subtracted from the gas spectra. To convert the absorbance of ozone to ozone concentration, 2950 $mol^{-1}cm^{-1}$ at 258 nm was used as the absorption coefficient of ozone in the gas and liquid phases [6].

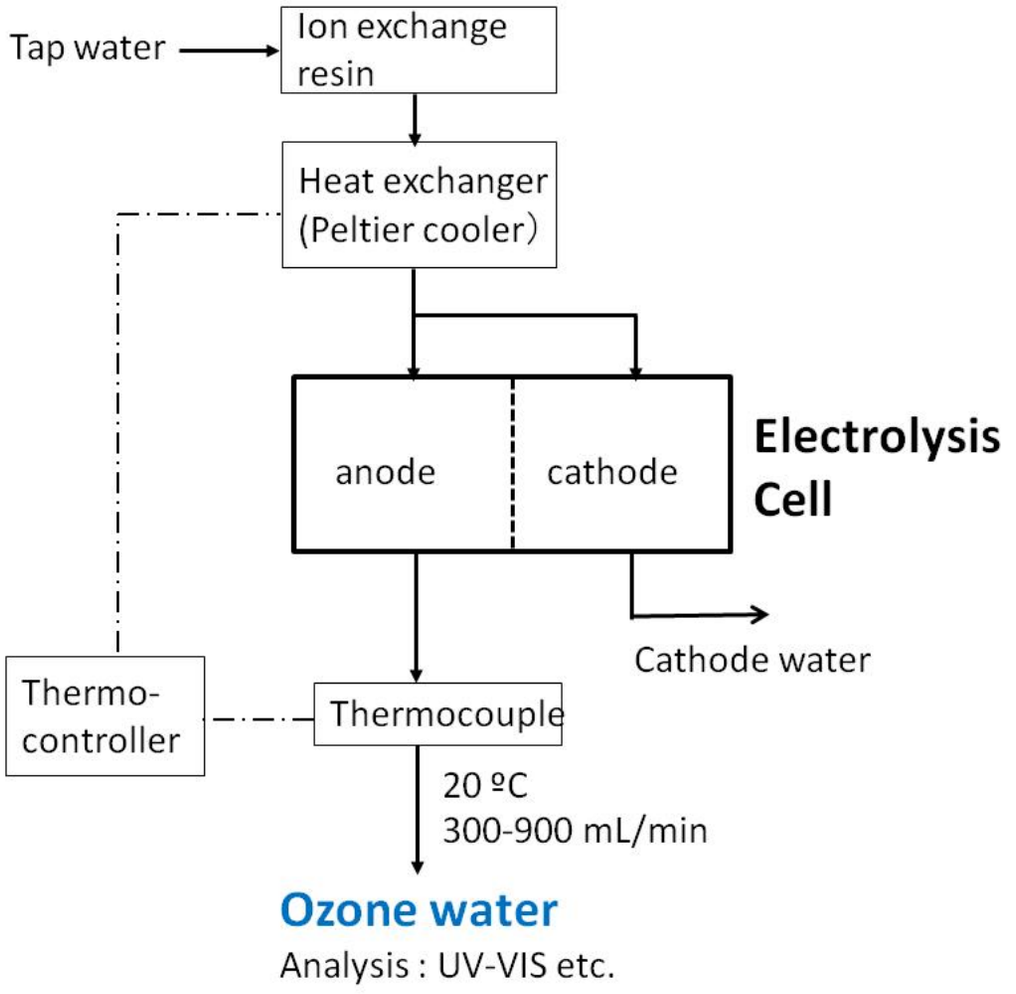

Figure 4. Flowchart of conventional EOP system

2.2. Efficiency of conventional electrolysis cell

The conventional cell can produce highly concentrated ozone water in the initial operation period. The obtained ozone water shows clear absorption by O_3. An example of O_3 decay in the anode water is shown in Fig. 5. In this experiment, O_3 electrochemically produced in the anode water was sampled in the optical cell, set in the UV-VIS absorptiometer, and measured of its decay every 10 min after the sampling time. As is evident from the spectra, ozone decay in the anode water is slow enough to neglect the sampling and scan times of the absorptiometer: The 1 min required for the absorption measurement does not affect the correct determination of ozone concentration. The typical half-life of ozone, 2 h in ion-exchanged water and 4 h in pure water, are in good agreement with those reported by Mizuno *et al*. [6].

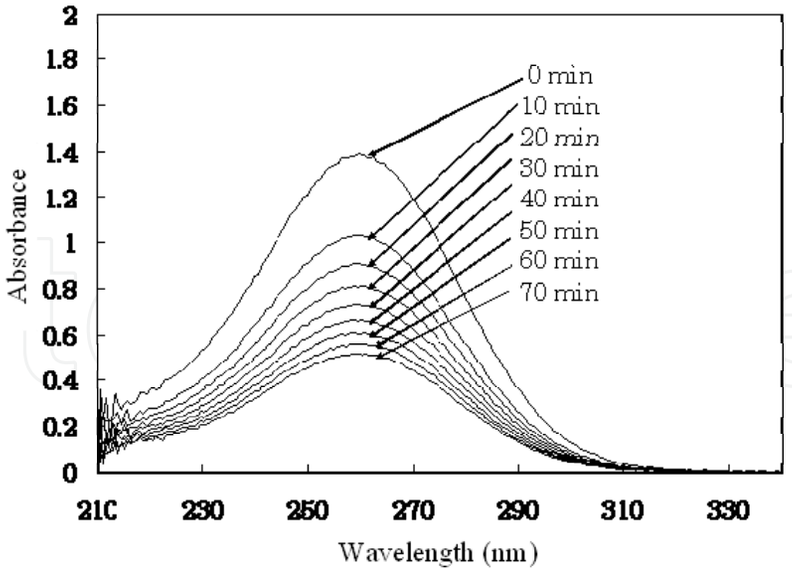

Figure 5. Time dependence of ozone absorption spectra [17]. Reproduced with permission from The Electrochemical Society.

To investigate the current efficiency of O_3 production with the conventional cell configuration and to check its run time dependence, ion-exchanged water was electrochemically decomposed in the cell at 5 A (0.625 A/cm^2) for 100 h. The flow rate of the anode water was 348 mL/min. The pH at the exit of the anode water was 6.0. The current efficiency of O_3 production in anode water is plotted as a function of run time in Fig. 6(a). No gas phase ozone was included in the efficiency calculation; only water-phase ozone was accounted for.

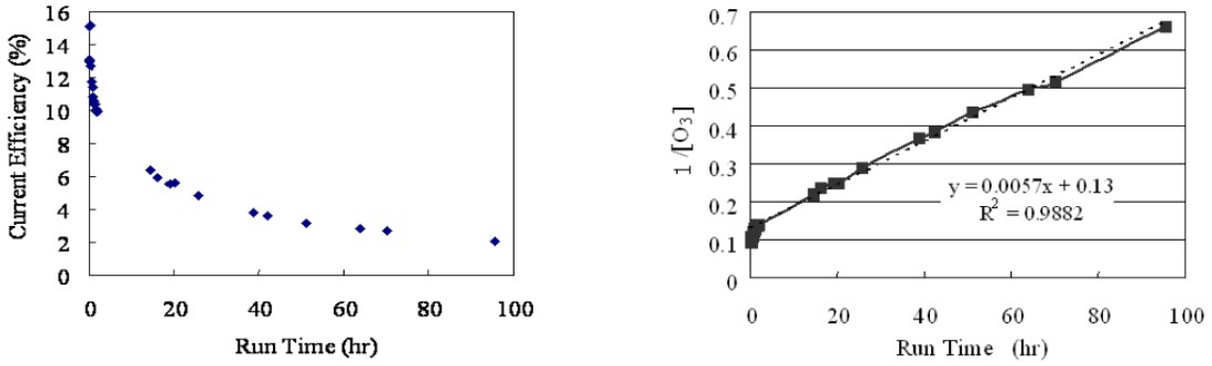

(a) Time dependence of current efficiency

(b) Time dependence of reciprocal O_3 concentration

Figure 6. Time dependence of efficiency and reciprocal O_3 concentration obtained using conventional cell [17]. Reproduced with permission from The Electrochemical Society.

As current efficiency decreased, voltage was increased from 6 V to 13 V during the experiment. The initial efficiencies of the system were markedly high: 13 to 15 % were observed in the first 1 h of operation. However, current efficiency decreased with run time to as low as 2 % after a 100 h operation. The initial ozone concentration was about 10 mg/L, but it decreased to 1.5 mg/L at the end of the run. It is clear that the lifetime of a

conventional cell is on the order of 10 h. The O_3 concentrations in Fig. 6(a) are converted to the reciprocal O_3 concentration, 1/[O_3] (L/mg), and are shown in Fig. 6(b). Such a figure is commonly used to estimate the order of reactions. The relation between 1/[O_3] and run time was found to be linear except for the initial 2-3 h of operation. A rapid degradation of the system occurs in the initial operation, and a steady degradation of the system starts after the rapid one. The linear increase in 1/[O_3] with run time after 2-3 h suggests the existence of a second-order reaction of the membrane with O_3 or its byproducts.

2.3. Mechanism of Nafion decomposition

The Nafion 117 membrane is a transparent film before the EOP operation. However, this membrane became black after the time dependence experiment. The image of the degraded Nafion 117 membrane is shown in Fig. 7. The cathode side of the membrane has a severely damaged (black) part and a slightly damaged (metallic silver) part.

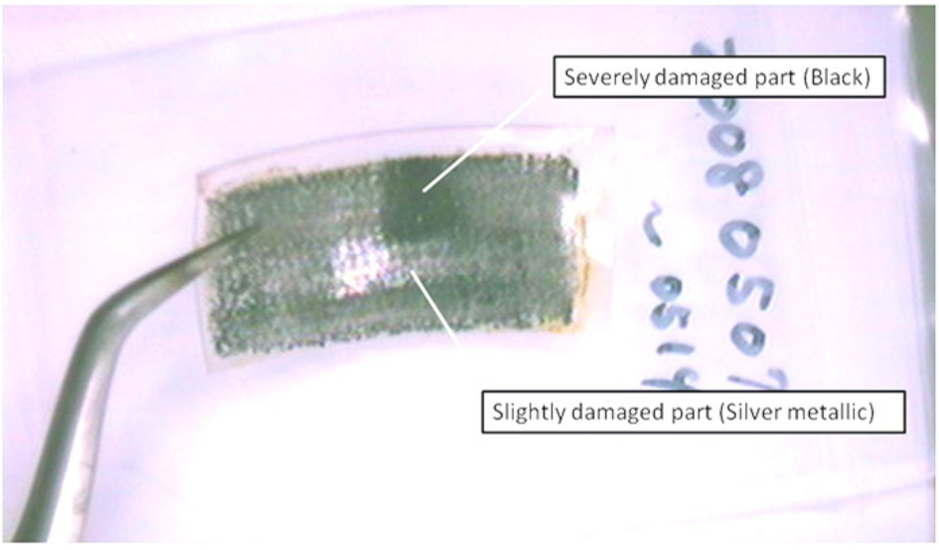

Figure 7. Degraded Nafion 117 membrane after 100-h operation at 0.625 A/cm^2 (view from cathode side).

FESEM images of the degraded Nafion 117 membrane are shown in Fig. 8. The anode side of the Nafion 117 membrane showed no morphological change, as shown in Fig. 8(a). However, holes were observed where the Nafion 117 membrane made contact with the Pt cathode, as shown in Fig. 8(b). The holes seem to be a result of the decomposition of the Nafion 117 membrane, and dendritic Pt nanoparticles were observed in the hole, as shown on the lower left side of Fig. 8(c).

EPMA measurements revealed that the Pt anode surface was covered with flakes of films consisting of Pt oxides, as shown in Fig. 9. The existence of Pt was also confirmed in the black region of the Nafion 117 membrane, but the composition could not be determined by EPMA because of the larger diameter of the probe beam of EPMA than of Pt nanoparticles. O, C, F and S signals originating from the Nafion 117 membrane also masked the real composition of Pt nanoparticles. However, semiquantitative XRF analysis indicated that the

Pt concentration on cathode side of the Nafion 117 membrane is about four times higher than that on the anode side. It is clear that the decomposition of the Nafion 117 membrane and the subsequent formation of holes decrease the efficiency of ozone production in the system.

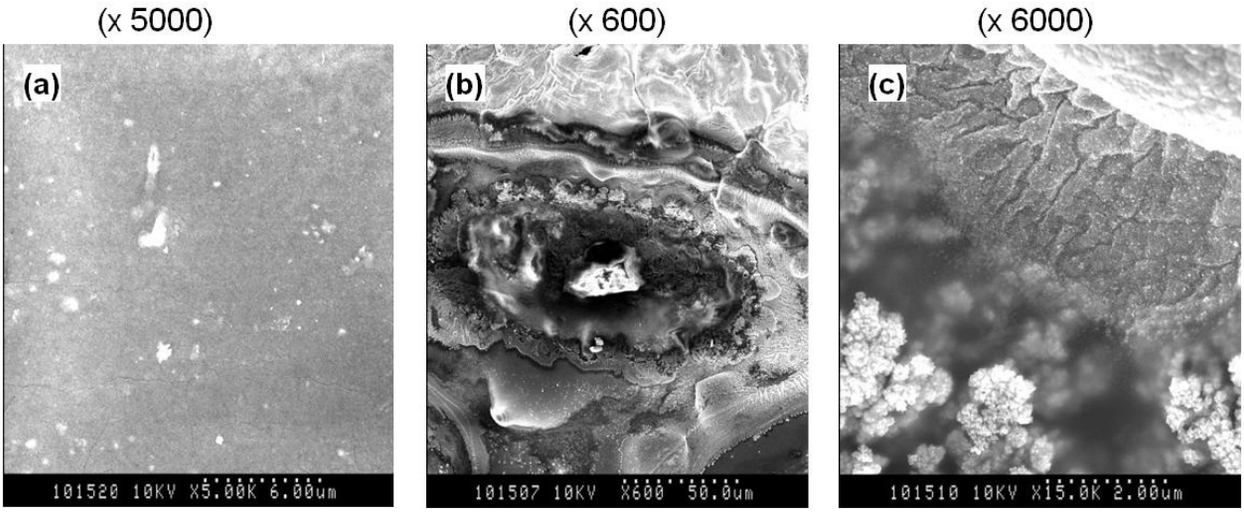

(a) Anode-side surface (b) Cathode-side surface (c) Inside hole of the cathode surface

Figure 8. FESEM images of degraded Nafion 117 membrane after time dependence experiment [17]. Reproduced with permission from The Electrochemical Society.

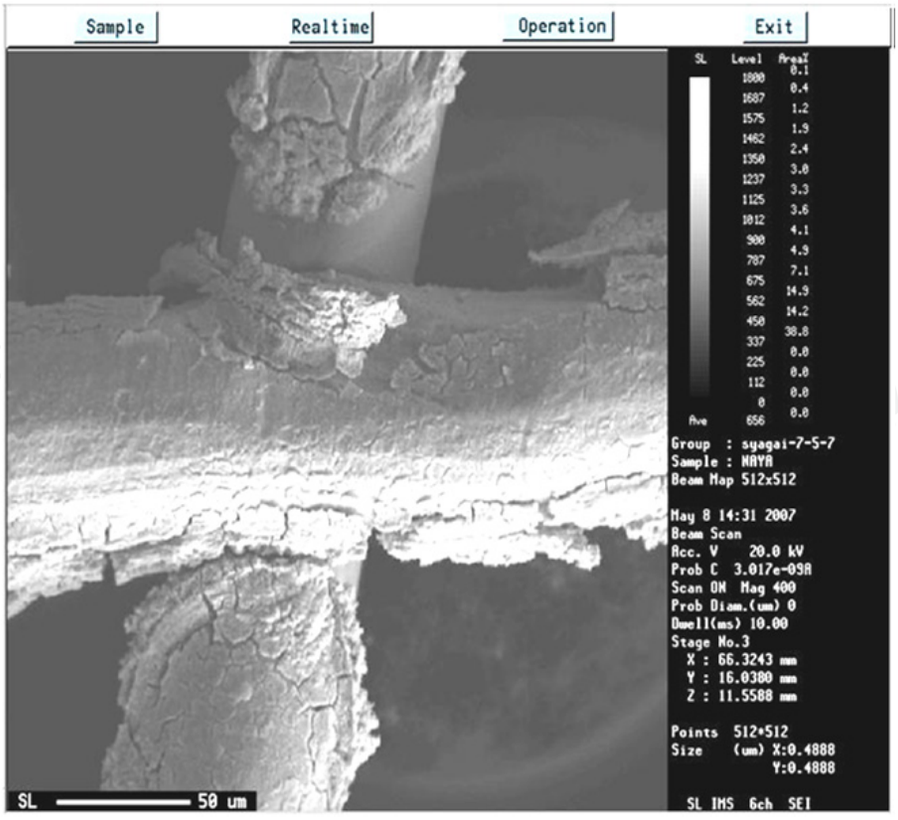

Figure 9. Surface of anode Pt mesh after time dependence experiment.

To determine the distribution of Pt black nanoparticles in the Nafion 117 membrane, four Nafion 117 membranes were set in the cell in piles, and the electrolysis of ion-exchanged water was performed for 50 h. A constant voltage of 12 V was applied, and current decreased from 17 A to 7 A according to the degradation of the cell. The ozone production efficiency calculated from the ozone concentration in the anode water was 10 % in the initial state, which decreased to 2 % at the end of the run. After the experiment, the Nafion 117 membrane on the anode side was light gray and almost transparent, but that on the cathode side was completely black. The sheets between them showed gradual tanning toward the cathode side.

From the above observations, we concluded that the rapid degradation is caused by the oxidation of the Pt anode to form Pt oxides, such as PtO_2. The formation of Pt oxides on the anode has been confirmed by the EPMA measurements. From the phase diagram of Pt in electrochemical equilibrium, PtO_2 and PtO_3 are expected to be stable substances in the electrolysis process where a voltage higher than 2 V is applied [19]. The poorer catalytic activity of Pt oxides than that of Pt probably decreases the current efficiency in this stage. During the oxidation of the Pt anode, ionic species, such as $Pt(OH)x^+$, can be formed where the local potential is in the range of 0-1 V, since Pt(OH) is also stable in this lower-potential region [19]. The ionic species could be released from the Pt anode surface, electrophoresed through the membrane, and concentrated on the cathode side of the Nafion 117 membrane. Finally, the ionic species are reduced by hydrogen and may work as a catalyst to decompose the Nafion 117 membrane by a mechanism similar to that reported in a fuel cell system [20]. An image of such a degradation mechanism is shown in Fig. 10.

H_2O_2 formed either in the self-decomposition process of O_3 or in the reduction of dissolved O_2 by H_2 should be a candidate source of ・OH radicals via Fenton's reaction on reduced Pt particles that are deposited on the cathode in contact with the Nafion membrane. To check the former possibility, O_3 self-decomposition simulation was performed using the WHD model [5]. A couple of the rate constants were adjusted to reproduce the O_3 decay profiles observed in our experiments (Fig. 5). The H_2O_2 concentrations calculated in the self-decomposition of saturated ozone water are very low: 4.38×10^{-12} mol/L at 1 sec and 4.35×10^{-11} mol/L at 10 sec. Moreover, the concentrations of H_2O_2 at 1 sec and 10 sec linearly increase with increasing initial O_3 concentration, and the second-order dependence of H_2O_2 formation with O_3 concentration cannot be reproduced. Therefore, it is clear that H_2O_2 formed via the self-decomposition of ozone is irrelevant to the degradation mechanism of the system.

The electrochemical generation of H_2O_2 during water electrolysis is reported by Kusakabe *et al.* [21] and Yamanaka *et al.* [22]. In particular, the Nafion 117 membrane was used as the solid polymer electrolyte, and the successful reduction of dissolved O_2 by H_2 to form H_2O_2 was reported in the latter's paper. Although the potentials applied in the latter's paper, 0-0.6 V, are much lower than those in our experiments, the inevitable formation of H_2O_2 can be expected in our system. Moreover, both the O_2 and H_2 concentrations should be

proportional to the O_3 concentration in our degraded system, since a lower O_3 production leads to a lower production of both O_2 and H_2. Therefore, the second-order formation of H_2O_2 with ozone concentration can be expected, and the second-order degradation of the system with ozone concentration can be explained by the electrochemical generation of H_2O_2.

Although we tried to check the H_2O_2 concentration in the cathode solution, the H_2O_2 concentration was too low to prove the existence of H_2O_2. The detectable limit of H_2O_2 in our lab is 0.02 mg/L, *i.e.*, $6x10^{-7}$ mol/L. A detailed elucidation of the degradation mechanisms of the system was not possible in this study. Therefore, we note the constants obtained from the linear part of Fig. 6(b) for future study: the intercept of the y-axis, which corresponds to the initial ozone concentration in the steady-degradation mode, was 7.7 mg/L; the slope, which indicates the rate constant of the second-order reaction of the Nafion 117 membrane with ozone, was 0.0057 L $mg^{-1} h^{-1}$.

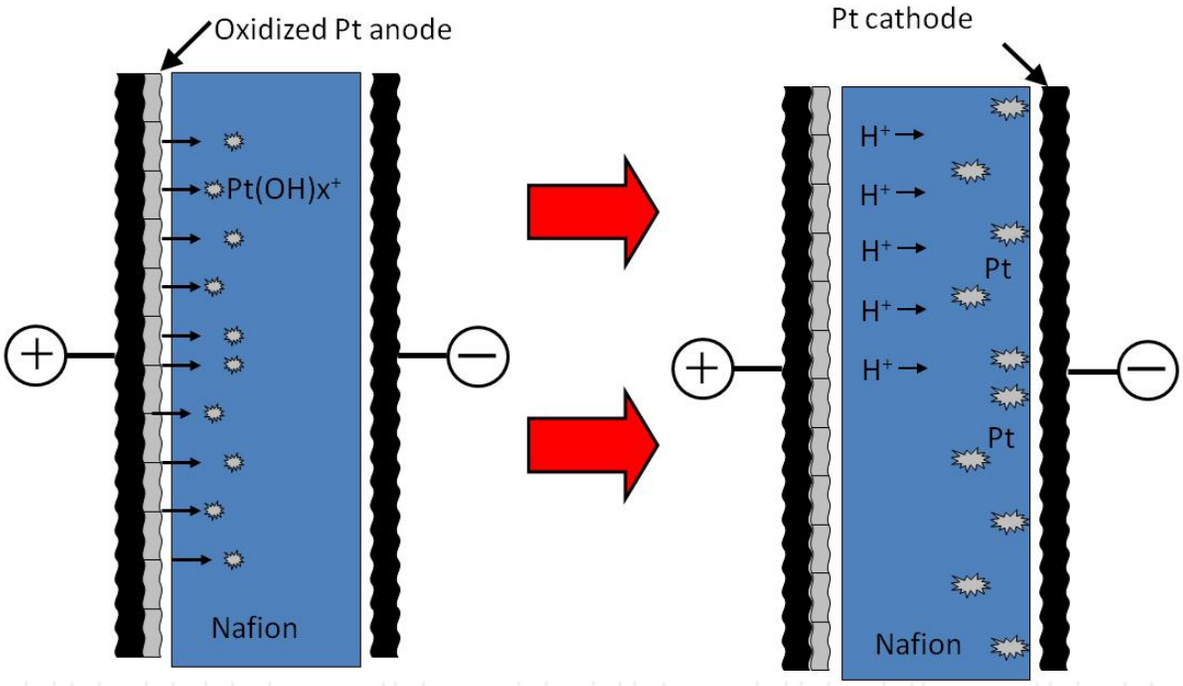

Figure 10. Mechanism of Nafion decomposition in electrolysis cell.

3. New EOP system

With the hypothesis that Pt nanoparticles deposited on the cathode side of the Nafion 117 membrane decompose the membrane, a new EOP cell was designed and tested for EOP operation. We inserted a quartz felt separator that captures Pt particles and prevents the degradation of the Nafion 117 membrane. Fundamental data for understanding the characteristics of the new electrolysis system were acquired during its first 50 h of operation, and the time dependence of current efficiency was measured in the subsequent experiment.

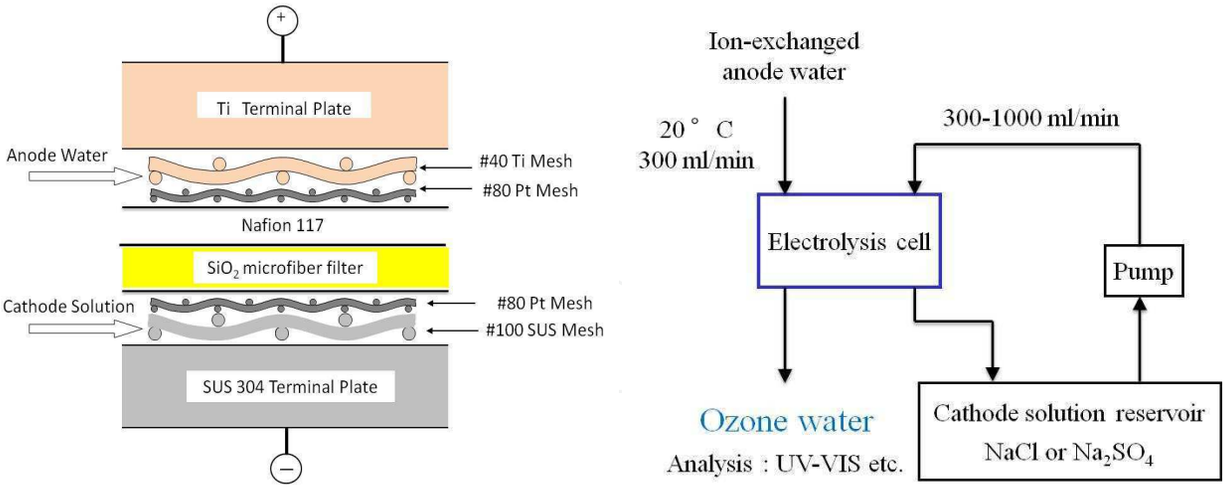

(a) Cross-sectional image of new electrolysis cell

(b) Flowchart of new electrolysis system

Figure 11. Configuration of new electrolysis system

3.1. Insertion of quartz felt separator

The new electrolysis cell consists of a Nafion 117 membrane and a quartz felt separator sandwiched by Pt #80 mesh electrodes. Two sheets of quartz filters (Whatman, QM-A 2-335-05) are stacked in piles, and used as the separator. The thickness of the separator is about 1 mm under ambient condition. The configuration of the new cell is illustrated in Fig. 11(a). The quartz filter is labeled as "SiO_2 microfiber filter" in the figure. To compensate for the low conductivity of the quartz separator, guaranteed reagent-grade NaCl and Na_2SO_4 (Kanto Chemical Co. Inc.) are used as cathode electrolytes (catholytes) without further purification. The purities of NaCl and Na_2SO_4 are more than 99 % and 99.5 %, respectively. These substances are dissolved in pure water, diluted to 0.01-1 M, and circulated through the cathode electrode at flow rates of 300-1000 mL/min by a water pump (Kamihata Fish Industries, Rio 50). The flowchart of the new system is shown in Fig. 11(b). The conductivities of the pure water and ion-exchanged water are 0.1 μS/cm and 240 μS/cm, respectively.

3.2. Characteristics of new EOP system

The O_3 production rates in the anode water and in the gas phase obtained with two catholytes are shown in Fig. 12(a) as functions of current. The current efficiencies calculated from these data in Fig. 12(a) are plotted in Fig. 12(b). In the case of 0.01 M catholytes, water electrolysis did not proceed. When the concentrations of NaCl and Na_2SO_4 were increased above 0.1 M, efficient water electrolysis was observed regardless of the solute and concentration. However, as is shown in Fig. 12(b), the current efficiencies at currents lower than 4 A obtained with Na_2SO_4 solutions were inferior to those obtained with NaCl solutions. Therefore, the 0.5 M NaCl solution was used in the time dependence experiment. The origin of such a discrepancy is further investigated, and explained in section 4. O_3 production rates in the anode water were about two times higher than those

in the gas phase regardless of the solute and concentration, and they showed a saturation behavior in the high-current region, while those in the gas phase increased in contrast [Fig. 12(a)].

Current efficiencies of more than 20 % were obtained at currents higher than 6 A. The efficiency is higher than those reported by other researchers who used Pt or PbO_2 electrodes, and close to that obtained using diamond electrodes. The power efficiency at 6 A and 7.74 V using the 0.5 M NaCl catholyte was 220 kWh/kg-O_3.

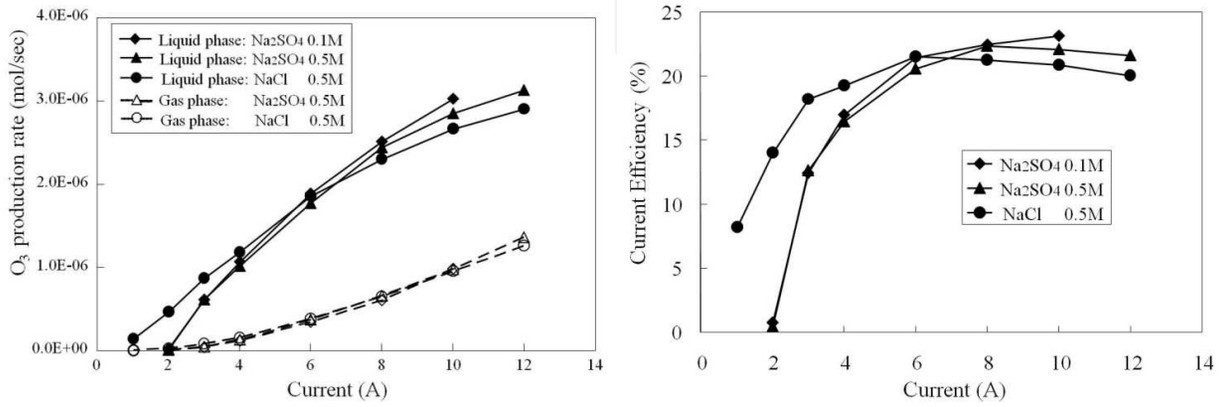

(a) O_3 production rates in liquid and gas phases

(b) Current efficiencies in O_3 production

Figure 12. O_3 production rates and current efficiencies of new electrolysis cell [17]. Reproduced with permission from The Electrochemical Society.

Since both current and power efficiency are functions of water flow rate and applied current, high efficiencies can be expected when water flow rate and current increase. An example of the relationship between water flow rate and current efficiency calculated from the ozone concentration in the anode water is shown in Fig. 13. In the experiments, the 0.5 M NaCl catholyte was circulated on the cathode side of the cell. Current efficiency increases with increasing water flow rate and current. At currents higher than 10 A, O_3 concentration starts to saturate in the anode water, and the differences in current efficiency become difficult to detect. If the water flow rate is increased to more than 1000 mL/min, and if O_3 becomes unsaturated in the anode water, the differences in current efficiency between 10 A and 14A would be apparent. A high voltage, such as above 7 V, applied to our system gave sufficient overpotential for O_3 production, and was probably one of the origins of good current efficiency. However, ozone concentration decreases with increasing water flow rate. Therefore, appropriate conditions should be chosen according to the required ozone concentration and water flow rate for practical use.

One of the possible efficiency loss is due to the solution resistance and/or contact resistance in the system. To measure such a loss, the overall applied voltage and potential difference between the Pt anode and cathode side of the Nafion 117 membrane were measured by placing electric wires on them using tiny Kapton tapes. The overall voltage and potential difference between the electrodes were measured at various currents using 0.5 M NaCl catholyte. Representative results are shown in Fig. 14. The potential difference between the

anode and cathode side of the membrane was roughly 30 % smaller than the overall voltage applied to the anode and cathode terminals of the cell. Since observable O_3 evolution occurs at a current of 1 A, as shown in Figs. 12 (a) and (b), nearly 4 V of the potential difference is required for EOP in the new system, suggesting that the involvement of the reaction in Eq. (3) is important for effective EOP.

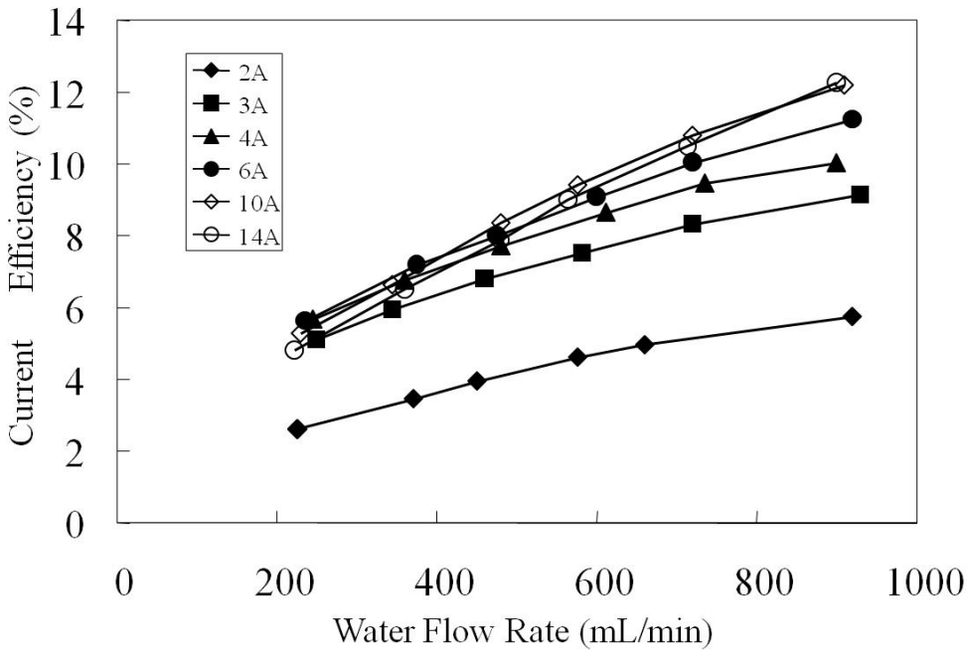

Figure 13. Current efficiency of O_3 formation in anode water as a function of water flow rate and current [17]. Reproduced with permission from The Electrochemical Society.

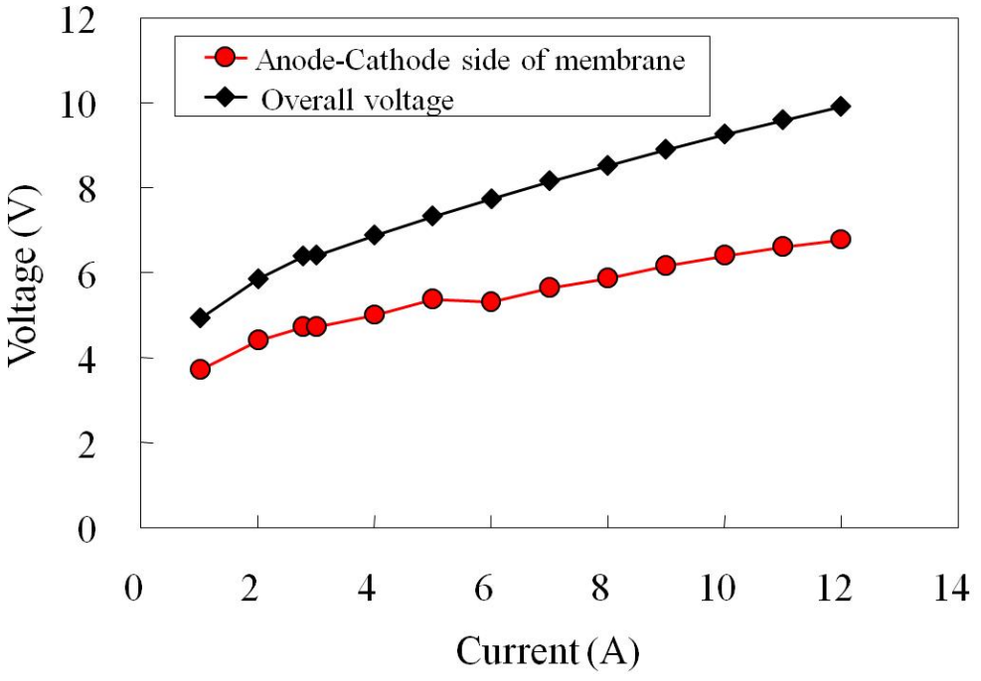

Figure 14. Relationship between applied voltage and potential difference of the electrodes

3.3. Lifetime of new system

After the characterization of the new system for 50 h, the accelerated degradation experiments were carried out using the 0.5 M NaCl catholyte. The flow rates of the anode water and catholyte were both 500 mL/min. A high current of 14 A was applied to accelerate the degradation of the system. The O_3 concentration in the anode water showed little degradation for 150 h of operation, as shown in the upper plots in Fig. 15. O_3 concentrations of 12 to 15 mg/L and a current efficiency of 18 to 20 % were maintained during the operation with a quartz felt separator. In this figure, the data in Fig. 6(a), which were obtained at a mild current of 5 A, are also plotted to compare the O_3 concentrations in the conventional and new cells. The separator works to maintain the high efficiency of the system and supports our hypothesis concerning the degradation mechanism. Provided that the degradation is a second-order process with O_3 concentration and that the O_3 concentration becomes one third at 4A compared with that at 14 A, as shown in Fig. 12(a), the lifetime at 4 A will be nine times longer than that at 14 A. Therefore, a stable operation of more than 1350 h (150 h multiplied by 9) could be expected under low-current operation.

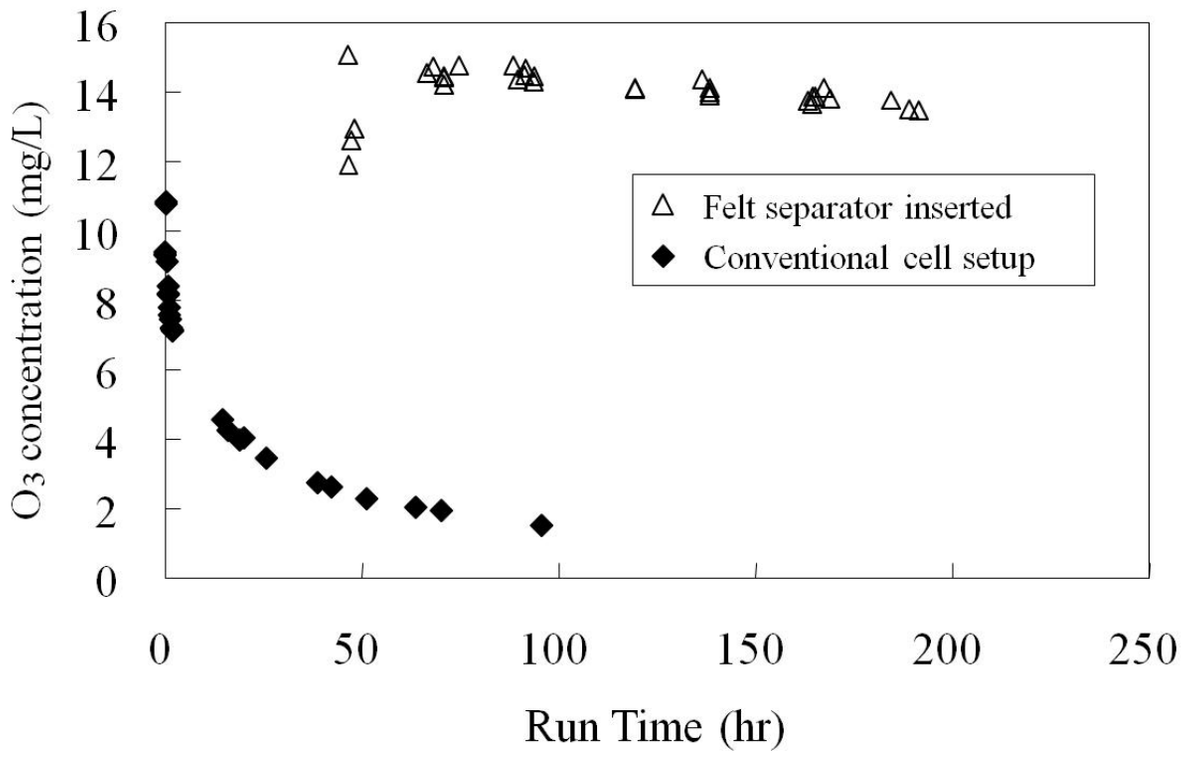

Figure 15. Run time dependence of O_3 concentration obtained in conventional and new cells [17]. Reproduced with permission from The Electrochemical Society.

The concentrations of ionic species in the anode water sampled in the middle of the run time dependence measurement were analyzed by ion chromatography (IC) and atomic absorption spectrometry (AAS), and the results are summarized in Table 1. Ion concentrations at the exit of the anode water were almost the same as those at the exit of the ion-exchange resin, *i.e.*, no significant change in ion concentration was detected except for small changes in Cl^- and Na^+ concentrations: Cl^- concentration slightly increased from 11.3 ppm at the exit of the ion exchange resin to 13.4 ppm at the exit of the anode water; on the other hand, Na^+ concentration decreased from 31.5 ppm at the exit of the ion exchange resin to 24.5 ppm at the exit of the anode water. The pHs of the anode water and cathode water in the middle of the run were 5.8 and 13.2, respectively. These changes were caused by the electrophoretic migration of ionic species.

The migration of the anode water associated with proton transfer through the membrane to the cathode side was also confirmed. The volume change in the circulated cathode solution was measured after operating for 42 h at 10 A. The volume increased from 1 L at the initial stage to 2 L after the operation. Therefore, the adjustment of the volume and pH of the cathode water is required at one or two day intervals during long runs of the system.

Ion	Tap water	Exit of ion-exchange resin	Exit of anode	(tw ppm) Method of analysis
Cl^-	11.5	11.3	13.4	IC
NO_3^-	8.1	7.7	7.8	IC
SO_4^{2-}	20.4	21.0	21.1	IC
Na^+	7.6	31.5	24.5	AAS
K^+	1.9	0.1	0.1	AAS
Mg^{2+}	4.0	0.0	0.0	IC
Ca^{2+}	19.9	0.0	0.0	IC
NH_4^+	0.0	0.2	0.2	IC

Table 1. Ion concentrations in tap water, exit of ion-exchange resin, and exit of anode water (IC: ion chromatography, AAS: atomic absorption spectrometry) [17]. Reproduced with permission from The Electrochemical Society.

4. Selection of catholyte

The key questions arising from the experiments in the above sections are as follows:

a. We noticed that the lifetime of the EOP system using the Na_2SO_4 catholyte is much shorter than that using the NaCl catholyte. How do these catholytes affect the lifetime of the system?
b. How does the NaCl catholyte concentration affect the efficiency and lifetime of the system?
c. The dissolution of the anode Pt electrode will be the limiting factor for the lifetime of the NaCl catholyte system after eliminating the problem of the decomposition of the membrane using the quartz felt separator. What is the dissolution rate of the Pt anode, and how long can the system be operated without changing the anode?
d. The contaminant concentrations in the ozone water produced from ion-exchanged water are lower than the allowable levels for drinking water. If pure water is introduced into the anode instead of ion-exchanged water, what will be the contaminant concentrations? Will the contaminants be at allowable concentrations for the sterilization of medical instruments and for the cleaning of electronic components?

To answer the above important questions, the dependences of catholyte composition and concentration on the efficiency and lifetime of the EOP system were investigated, and the dissolution rate of the Pt anode and the contaminant concentration in ozone water were measured. All the experiments were carried out using pure anode water instead of ion-exchanged water, because the analysis of ions that migrated from the catholyte to the anode Pt surface seemed to be essential to understand the effects of the catholyte on the efficiency and lifetime of the system. The other experimental setup and measurements used are the same as these in the last section (see Fig. 11).

4.1. Effects of catholytes on EOP efficiency

Pure water produced by passing tap water through Na-type ion-exchange resin (Rohm and Haas, Amberlite IR-120B Na) and reverse osmosis (Dow Chemical, FILMTEC TW30-2514) is introduced into the anode at a flow rate of 300 mL/min. The conductivity of the pure water is less than 0.1 μS/cm. The residence time and flow speed of the anode water in the cell are estimated to be 0.085 s and 0.94 m/s, respectively. The O_3 concentrations obtained using 0.5 M NaCl and 0.5 M Na_2SO_4 catholytes as functions of current density are shown in Figs. 16(a) and (b), respectively. In these experiments, current was slowly increased and held for 20 min to stabilize the system at each measurement point. Therefore, 2 h was required to obtain a series of NaCl or Na_2SO_4 data. The holding time should be long enough to observe the degradation of the system, if any.

When the NaCl catholyte was used, the O_3 concentrations in the anode water and gas phase increased with current, as shown in Fig. 16(a). The concentration of ozone water was higher than 20 mg-O_3/L-water (mg/L) at a current higher than 1 A/cm^2 (8.0 V); and it was 24.8 mg/L at 1.25 A/cm^2 (9.1 V). On the other hand, the O_3 concentrations obtained using the Na_2SO_4

catholyte were lower than those obtained using the NaCl catholyte in the entire current range in Fig. 16(b). No O_3 concentration in the anode water higher than 20 mg/L was obtained using the Na_2SO_4 catholyte. Moreover, the O_3 concentrations in the anode water and gas phase decreased at 1.25 A/cm^2, suggesting that the system was degraded within 2 h of the measurement.

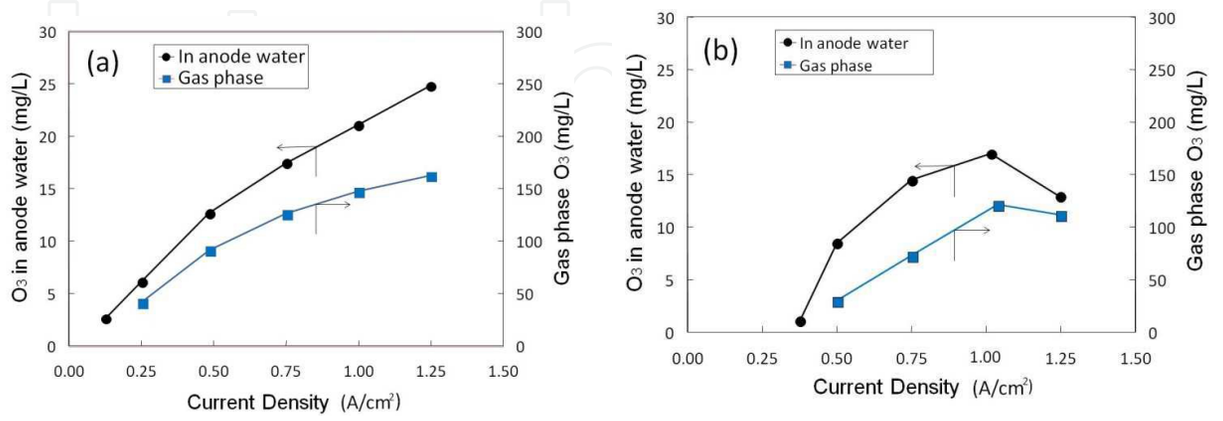

(a) 0.5 M NaCl catholyte (b) 0.5 M Na_2SO_4 catholyte

Figure 16. O_3 production rates in anode water and gas phase

The current efficiencies calculated from the data in Fig. 16 are plotted in Figs. 17. As seen in Fig. 17(b), the current efficiencies obtained using the Na_2SO_4 catholyte were lower than those obtained using the NaCl catholyte [Fig. 17(a)]. Although the electric conductivity of a Na_2SO_4 electrolyte, 8.23 Sm^{-1}, is higher than that of a NaCl electrolyte, 7.06 Sm^{-1}, at 1 M and 20 ºC, no improvement in current efficiency was observed in the experiments. The origin of the differences observed in the EOP efficiencies caused by changing the catholyte will be discussed in section 4.4.

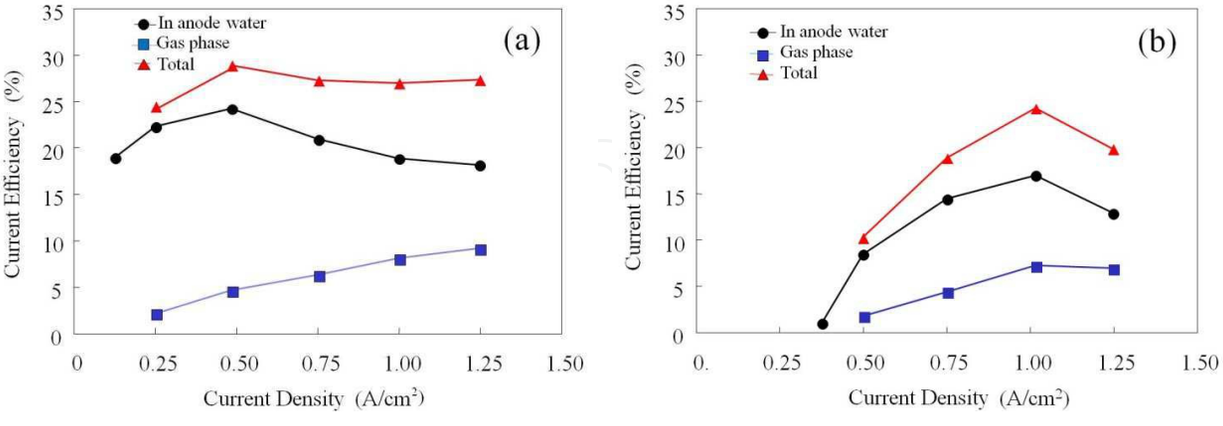

(a) 0.5 M NaCl catholyte (b) 0.5 M Na_2SO_4 catholyte

Figure 17. Current efficiency of O_3 production

The current efficiencies shown in Fig. 17(a) were higher than those reported in the previous data in section 3.2. The current efficiency of 29 % at 0.5 A/cm^2 (6.6 V) was markedly high, and efficiencies higher than 25 % were obtained in the entire current range. The O_3 production

rates in the anode water and gas phase at 0.5 A/cm^2 were measured to be 274 mg/h and 52 mg/h, respectively. From these data, the power efficiency of the system at 0.5 A/cm^2 was determined to be 76 kWh/kg-O_3, which is lower than that (220 kWh/kg-O_3) obtained in a previous experiment and those reported using other anode materials in EOP systems. The theoretical electric power required for a perfect EOP system is estimated to be 5.06 kWh/kg-O_3, supposing 100 % consumption of the current for producing O_3 and the standard voltage of O_3 formation, 1.511 V. Further improvement in power efficiency is possible by introducing other measures, such as O_2 gas recycling into the cathode water [23]. However, the cost of electricity is reasonably low even in the present EOP system. The NaCl catholyte system can produce 1 kg-O_3 at an electricity cost of 7 US dollars assuming that the price of electricity is 10 cents/kWh. 100 kL of 10 mg/L-ozone water will be produced from 1 kg-O_3.

4.2. Effects of catholytes on lifetime

To observe the time dependence of the O_3 concentration and to check the morphological change of the Pt anode after a long operation, accelerated degradation experiments were performed. During the experiments, the flow rates of the anode water and the catholytes were both set to 300 mL/min, and a high current of 1.25 A/cm^2 (10 A) was applied to accelerate the degradation. The concentrations of the NaCl and Na_2SO_4 catholytes were set to 0.5 M. The concentrations of Na^+, Cl^- and SO_4^{2-} in the anode water were measured in the middle of the accelerated-degradation experiments, and are summarized in Table 2.

Ion	Na_2SO_4 0 A	Na_2SO_4 10 A	NaCl 10 A	(wt ppm) Method of analysis
Cl^-	0.06	0.01	7.4	IC
SO_4^{2-}	0.14	1.15	-	
Na^+	0.11	-	0.02	
K^+	0.04	-	-	
Ca^{2+}	0.02	0.01	0.01	
NH_4^+	0.01	0.01	0.01	
Pt	0.023 wt ppb	0.13 wt ppb	0.62 wt ppb	ICP-MS

Table 2. Impurity concentrations in anode water sampled during electrolysis at 0 A and 10 A using the Na_2SO_4 and NaCl catholyte. (Method of analysis: IC, ion chromatography; ICP-MS, inductively coupled plasma mass spectrometry)

The ion concentrations at the exit of the anode water sampled at 0 A/cm^2 using the Na_2SO_4 catholyte should be the same as those in pure water, except for slight increases in SO_4^{2-} and Na^+ concentrations. These ions came from the catholyte by diffusing through the Nafion 117 membrane. SO_4^{2-} concentration increased to 1.15 wt ppm at an electrolysis current of 10 A (1.25 A/cm^2) using the Na_2SO_4 catholyte. Cl^- concentration also increased to 7.4 wt ppm, and Na^+ concentration decreased to 0.02 wt ppm at 10 A (1.25 A/cm^2) using the NaCl catholyte. These changes were caused by the electrophoretic migration of these ionic species.

The results of the degradation experiments are shown in Fig. 18. Note that the O_3 production in the gas phase is not included in the plots. When the 0.5 M NaCl catholyte was used, the O_3 concentration showed only a slight degradation during the operation for 130 h, as is shown in the upper plots in Fig. 18. A high O_3 concentration ranging from 20 to 25 mg/L was maintained during the experiment (the Cl^- concentration in the anode water was 7.4 ppm). The slight decrease in the concentration is probably due to the dissolution of the Pt anode electrode resulting in poor contact between the anode and the Nafion 117 membrane. However, the use of the 0.5 M Na_2SO_4 catholyte caused a rapid decrease in O_3 concentration: The initial concentration of 18 mg/L decreased to 7 mg/L after operating the system for 60 h, as shown in the lower plots in Fig. 18. In this experiment, only 0.01 wt ppm Cl^- was found in the exit of anode water. The degradation data reported in section 3.3 using ion-exchanged water and the 0.5 M NaCl catholyte are also shown in the middle plots in Fig. 18. A stable EOP was observed in our previous experiment (the SO_4^{2-} and Cl^- concentrations in the anode water were 21.1 ppm and 13.4 ppm, respectively) [17].

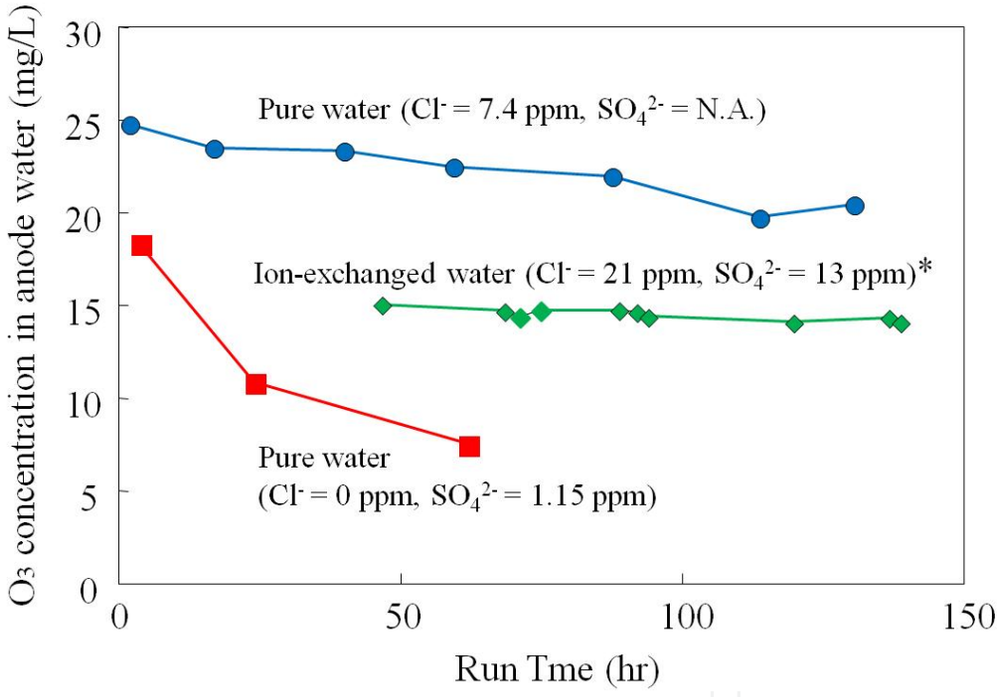

Figure 18. Run time dependence of O_3 concentration in anode water. The data set indicated by "*" is the same as that in Fig. 15.

After the accelerated-degradation experiments, the anode surface in contact with the Nafion 117 membrane became brown when the 0.5 M Na_2SO_4 catholyte was used. In contrast, the anode surface was clean and only a small portion of that in contact with the Nafion 117 membrane became yellow when the 0.5 M NaCl catholyte was used. SEM images of the Pt anode electrodes after the degradation experiments are shown in Fig. 19. As is clear in Fig. 19(c), the surface of the anode electrode in contact with the Nafion 117 membrane was covered with an approximately 10-μm-thick oxide layer, when the

system was operated using the 0.5 M Na_2SO_4 electrolyte. The surface of the anode electrode remained clean [Fig. 19(a)], and only a thin layer of oxide deposit was observed in a small area [Fig. 19(b)], when the system was operated using the 0.5 M NaCl catholyte.

The above oxide layers were assigned to amorphous PtO_2 (a-PtO_2) by microscopic Raman spectroscopy, in which the characteristic broad spectrum of a-PtO_2 peaking at 600 cm^{-1} with an FWHM of 200 cm^{-1} was observed. No sharp peak originating from PtO or α-PtO_2 crystals was observed [24]. EDX measurements indicated that 3.5 wt % Cl was present in the a-PtO_2 layer formed using the 0.5 M NaCl catholyte [Fig. 19(b)]. Because our EDX apparatus could not detect oxygen, the rest of the material measured in the oxide layer was 96.5 wt % Pt. No Cl was observed in the oxide layer formed using the 0.5 M Na_2SO_4 catholyte. The high concentration of Cl adsorbed onto the a-PtO_2 layer suggests that Cl^- that migrated on the anode surface inhibited the formation of the a-PtO_2 layer. When chloride is added to a sulfuric medium, its adsorption inhibits the formation of oxide films in the low-voltage range, *i.e.*, at voltages lower than 1.5 V vs RHE [25, 26]. Because the anode voltages applied in our EOP system were much higher than those in the literature, a more efficient adsorption of chloride is expected.

SEM images of the captured Pt particles on the cathode side of the quartz separator are shown in Fig. 20. Small and spinous Pt particles were captured in the separator using the 0.5 M NaCl catholyte, as shown in Fig. 20(a). On the other hand, granular Pt aggregates were observed using the 0.5 M Na_2SO_4 catholyte, as shown in Fig. 20(b). The difference in the shape of the captured Pt particles suggests that the precursors of the particles may be different. However, further analysis should be required to determine the origin of the difference in the shape of the captured Pt particles.

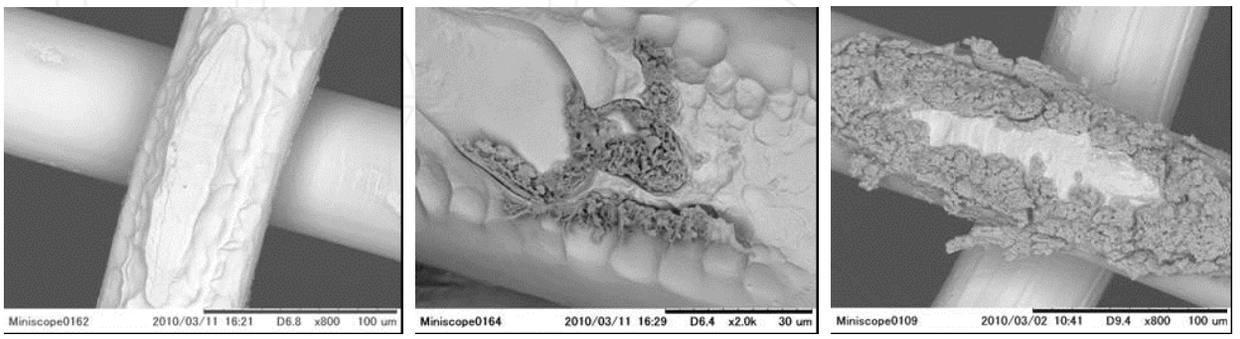

(a) Clean part (0.5 M NaCl catholyte) (b) Yellow part (0.5 M NaCl catholyte) (c) Brown part (0.5 M Na_2SO_4)

Figure 19. SEM images of Pt anodes after accelerated degradation experiments

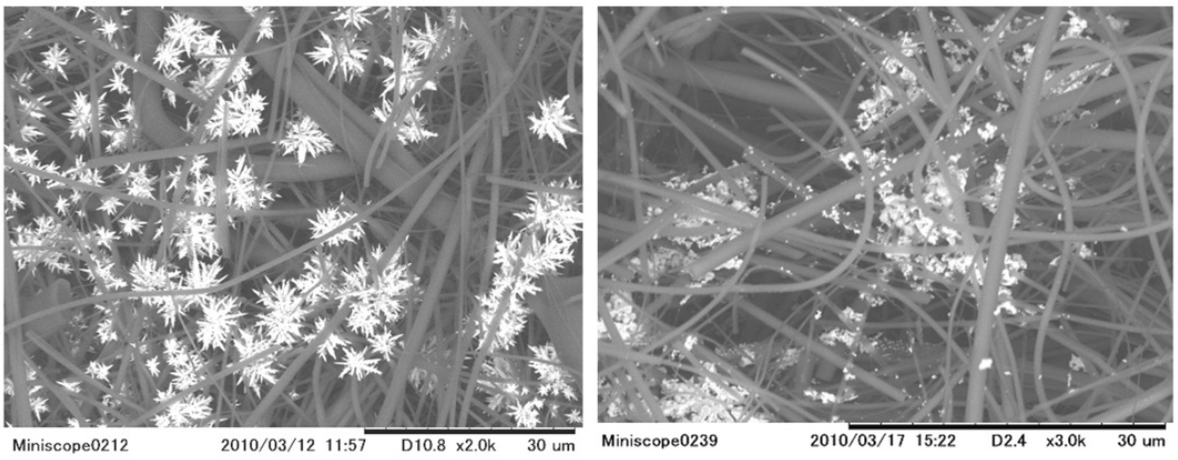

(a) 0.5 M NaCl catholyte (x 2,000) (b) 0.5 M Na_2SO_4 catholyte (x 3,000)

Figure 20. SEM images of captured Pt particles in quartz felt separator

4.3. Effects of NaCl concentration

The effects of catholyte concentration on the current efficiency and lifetime of EOP were measured by changing the NaCl catholyte concentrations from 0.003 M to 0.085 M. These measurements were performed at a constant current density of 0.625 A/cm^2 (5 A) for 20 h. The results are shown in Fig. 21. The current efficiency of EOP increases with increasing concentration of the NaCl catholytes probably owing to the increase in catholyte conductivity. The decrease in the current efficiency with run time was observed for NaCl concentrations lower than 0.028 M. The efficiency linearly decreases with run time using these dilute catholytes. However, in the case of the 0.085 M catholyte, the degradation speed of the system became lower, and the efficiency was kept higher than 23 % for 20 h. This efficiency is similar to that obtained using the 0.5 M NaCl catholyte [Fig. 17(a)], and the low degradation speed is indicative of the realization of the long and stable operation of the system. Therefore, a NaCl concentration higher than 0.085 M is adequate for the EOP system.

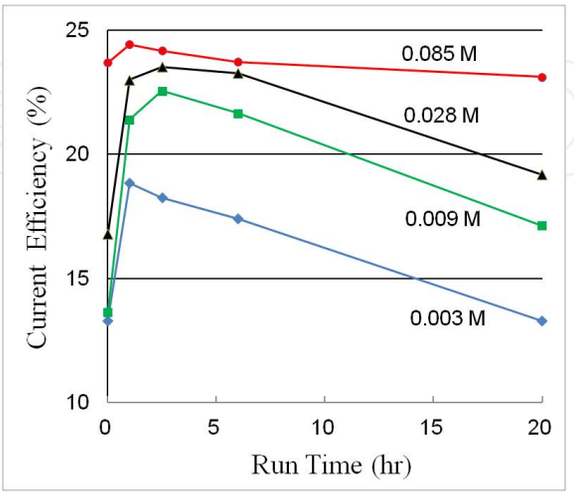

Figure 21. Concentration dependence of catholyte on the efficiency and lifetime measured at 0.625 A/cm^2 (5 A).

4.4. Inhibition mechanism of Pt oxide formation

From these observations, we conclude that Cl^- that migrated from the catholyte to the anode surface inhibited the formation of the a-PtO_2 layer. As a result, the anode surface was kept clean during the accelerated degradation experiments. The poor performance of the system using the Na_2SO_4 catholyte, shown in Figs. 16(b), 17(b) and 18, suggests that the anodes were rapidly oxidized from the beginning of the experiments owing to the absence of Cl^-. Therefore, Cl^- that migrated from the catholyte to the anode surface is indispensable for a long and stable operation of the EOP system, whereas SO_4^{2-} concentration is probably irrelevant for long lifetime as long as sufficient amount of Cl^- is supplied to the anode, as shown in the middle plots in Fig. 18.

The standard electrode potentials for chlorination and oxidation reactions of Pt are as follows [27]:

$$Pt + 4Cl^- \rightarrow \left[PtCl_4\right]^{2-} + 2e^- \qquad E^0 = 0.758\ V \tag{14}$$

$$\left[PtCl_4\right]^{2-} + 2Cl^- \rightarrow \left[PtCl_6\right]^{4-} + 2e^- \quad E^0 = 0.726\ V \tag{15}$$

$$Pt + H_2O \rightarrow PtO + 2H^+ + 2e^- \qquad E^0 = 0.980\ V \tag{16}$$

$$PtO + H_2O \rightarrow PtO_2 + 2H^+ + 2e^- \qquad E^0 = 1.045\ V. \tag{17}$$

Because chlorination reactions take place at lower potentials than oxidation reactions, Pt is chlorinated, ionized, and dissolved in anode water in the presence of Cl^- ions. Thus, the formation of Pt oxide films can be inhibited.

If the efficiency of the system is degraded by the formation of the a-PtO_2 layer on the anode surface using the Na_2SO_4 catholyte, an important question arises: Does the a-PtO_2 layer have a lower catalytic activity than Pt in EOP reactions? The formation mechanisms and resultant structures of oxide layers on a Pt anode have been extensively studied to understand the electrocatalytic properties of such layers [28-34]. Pt oxide layers are considered to have slightly beneficial effects on oxygen evolution reactions. Shibata reported that the oxidation treatment of a Pt anode surface with 1 M H_2SO_4 solution for 28 h enables a stable electrolysis activity of the Pt anode for more than 30 h [28]. Tremiliosi-Filho *et al.* reported that the rate of O_2 evolution increases with the period of oxide film formation at various electrolysis potentials [33]. Gottesfeld *et al.* found that Pt oxide films formed after a long-term polarization of potential between 2.1-2.25 V vs. RHE in 0.5 M H_2SO_4 solution could be identified as film β (it is now assigned to a-PtO_2), and that the films shows good electric conductivity as well as an improvement in the performance of oxygen evolution reaction with the lowering of the oxygen evolution voltage from 2.1 V to 2.0 V at a current of 10 mA/cm² [31]. Therefore, we did not concern ourselves with the negative effect of Pt oxides on EOP reactions.

If Pt oxide layers significantly decrease oxygen overpotential in water electrolysis reactions and lead to higher O_2 evolution, the efficiency of O_2 formation would increase and the negative effect on EOP could be expected. To determine the effects of a-PtO_2 layers on EOP, we are now conducting experiments to measure the electric properties and electrocatalytic activities of a-PtO_2 layers by fabricating such layers on the Pt anode. We have found that a-PtO_2 layers have a much lower catalytic activity than pure Pt in EOP reactions; the results will be reported soon [35].

4.5. Current balance

The current balance of the 0.5 M NaCl catholyte system was measured and checked by comparing the calculated currents for O_3 production in the anode water and gas phase as well as those for O_2 production. In this experiment, the concentration of dissolved O_2 in anode water was measured using an electrochemical O_2 sensor (Hach Ultra, Orbisphere 3600 and 31124). The O_2 sensor was calibrated to match the current balance of the system at high current density operation. The gas phase O_2 production rate was obtained by subtracting O_3 production from the overall anode gas production. To double-check the current balance, we tried to measure H_2 production rate. However, it was not possible to capture H_2 gas in a cylinder, because H_2 formed very tiny bubbles that dispersed in the catholyte. Current balances calculated at seven currents are summarized in Fig. 22. The calculated currents are in good agreement with the measured ones, *i.e*, the 100 % line in Fig. 22, except that in the current range lower than 0.25 A/cm^2, where the low gas production rates could be the source of error. As is clear from Fig. 22, the system has neither an apparent current leakage nor markedly abundant products other than O_3, O_2, and H_2. More than 70 % of the current was consumed in producing O_2. It is also clear from Fig. 22 that the current consumption for O_2 formation in anode water decreases with applied potential, while that for O_3 formation in gas phase and anode water increases. Therefore, it is suggested that the oxidation of O_2 in anode water to O_3 [Eq. (3)] is the dominant process for O_3 formation. However, more detailed kinetic studies on O_2 and O_3 formation reactions, such as the branching ratio of Eqs. (2) and (3), will be required for the further understanding of the system.

4.6. Pt dissolution rate and lifetime of new system

The weight of the Pt anode mesh was about 0.4 g before the experiments. They decreased by 5.4 mg and 7.7 mg, corresponding to dissolution rates of 5.4 μg/Ah and 6.9 μg/Ah, after the accelerated experiments using the Na_2SO_4 and NaCl catholytes, respectively. These values are in agreement with the reported one, 5 μg/Ah, in which the corrosion rate of the Pt electrode with a 1 cm^2 surface area was measured in the H_2SO_4 electrolyte up to 1 M [36]. It is clear from Fig. 19(a) that the anode surface in contact with the Nafion 117 membrane dissolved during the operation, and that the surface area of our Pt anode mesh in contact with the Nafion 117 membrane was also on the order of approximately 1cm^2. Although the accuracy was not sufficient for the precise comparison of Pt concentrations in anode water listed in Table II because of the infinitesimal quantity of Pt determined by ICP-MS, the

tendency coincides with the results of the weight measurements: The Pt concentration obtained using the 0.5 M NaCl catholyte is higher than that obtained using the 0.5 M Na_2SO_4 catholyte. From these observations it can be assumed that the Pt anode dissolves in anode water faster when the NaCl catholyte was used than when the Na_2SO_4 electrolyte is used. In the case of electrolysis using the NaCl catholyte, Pt mass balance calculation indicates that 20 % of the dissolved Pt is carried out of the system in anode water, and the rest of the dissolved Pt diffuses and migrates to the cathode side. The lifetime of the system can be estimated in terms of Pt weight loss that leads to poor contact between the anode and the Nafion 117 membrane. Because the Pt anode is pressed against the membrane surface using a Ti #40 mesh and a Ti terminal plate, the contact can be maintained fairly well when the Pt weight loss is small. If a 10 % loss in Pt weight is allowed to maintain good contact, the system can be operated up to a weight loss of 40 mg which corresponds to an operation period of 5800 Ah, *i.e.*, 2900 h of operation at 0.25 A/cm^2, using the NaCl catholyte. 6 mg-O_3/L ozone water will be obtained at a current density of 0.25 A/cm^2, and the system can be operated for 8 h a day for 365 days without changing the anode.

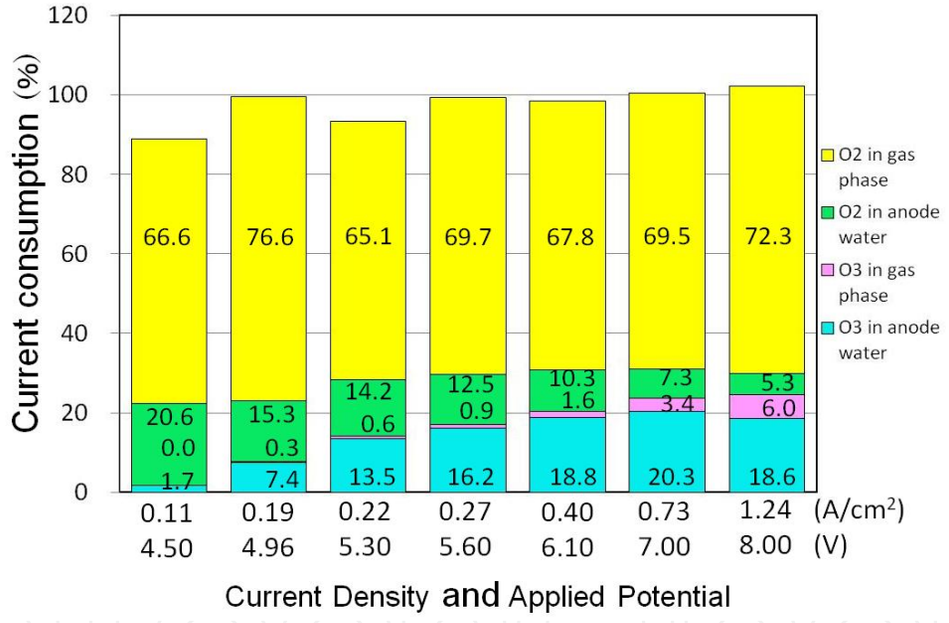

Figure 22. Current consumption balances calculated from production rates of O_3 and O_2 (0.5 M NaCl catholyte was used).

5. Impurities in ozone water

Impurity levels in the exit of the anode water obtained using ion-exchanged water are comparable to those in drinking water, as shown in Table 1. Therefore, ozone water should be safe enough for family use, such as gargles and washing hands. On the other hand, the concentrations of the impurities listed in Table 2, such as Na^+, Ca^{2+}, and NH^{4+} in anode water using the 0.5 M NaCl catholyte, are on the order of 0.01-0.02 wt ppm. They are much lower than those in ion-exchanged water (see Table I). The ozone water obtained in the pure water system consists of highly concentrated O_3 and 7.4 wt ppm Cl^-. Therefore, ozone water can be

used in various processes, such as the sterilization of medical instruments. Because Cl^- is undesirable in the cleaning processes of electronic components, Cl^- washout will be required after using the ozone water for such processes.

6. Conclusion

The efficiency of ozone production using a conventional Pt electrode system decreased with run time. The linear increase in $1/[O_3]$ with run time after 2-3 h suggests the existence of a second-order reaction of the Nafion 117 membrane with ozone or its decomposition products. The degradation was caused by Pt particles concentrated on the cathode side surface of the Nafion 117 membrane. The particles catalyze the reaction between the Nafion 117 membrane and ozone to produce holes on the membrane's cathode side surface. To prevent the decomposition of the membrane, a quartz felt separator was inserted between the Nafion 117 membrane and the cathode electrode. As a result, a high current efficiency of more than 20 % and a lifetime longer than 150 h have been achieved in the new electrolysis system. The quartz felt separator succeeded in capturing Pt particles and preventing the membrane from decomposition.

Then the effects of the NaCl and Na_2SO_4 catholytes on the current efficiency and lifetime of the new EOP system were investigated using pure anode water. When a 0.5 M NaCl catholyte was used, a high current efficiency of 29 % and a high power efficiency of 76 kWh/kg-O_3 were achieved at an electrolysis current of 0.5 A/cm^2 (6.6 V). The accelerated degradation experiments indicated that the combined use of pure anode water and the 0.5 M NaCl catholyte kept the Pt anode surface clean and enabled an efficient operation longer than 130 h. On the other hand, the Pt anode surface in contact with the Nafion 117 membrane was covered with a 10-µm-thick a-PtO_2 film and the efficiency decreased from 13 % to 5 % after the accelerated experiments for 60 h using the Na_2SO_4 catholyte. It is suggested that the formation of a-PtO_2 films decreases the electrocatalytic activity of the Pt anode in the O_3 formation reaction. The NaCl concentration dependence measurements indicate that NaCl concentrations higher than 0.085 M will be adequate for the EOP system. Pt dissolution rates of 5.4 µg/Ah and 6.9 µg/Ah were measured using the Na_2SO_4 and NaCl catholytes, respectively. If a 10 % loss in Pt weight is allowed to maintain good contact between the anode and the Nafion 117 membrane, the system using the NaCl catholyte can be operated for 5800 Ah, *i.e.*, 8 h per day for 365 days at 0.25 A/cm^2 without changing the anode. The long lifetime, good current and power efficiencies, very low impurity concentrations, the compactness of equipment and low-voltage operation achieved by the new system will enable a wide expansion of the application of ozone water.

7. Future research

Important breakthroughs remain to be achieved. The authors plan to develop the following advanced EOP technologies: a direct tap water electrolysis system that does not require the use of ion-exchange resin or reverse osmosis; a once-through catholyte flow system that can

eliminate the formation and discharge of a strongly alkaline catholyte solution; an effective utilization system of gas phase ozone; a new and effective anode catalyst system. Such kinds of improvements will be achieved soon, because we have ideas and strategies for realizing advanced systems.

To clarify the effectiveness of ozone water for sterilization processes, we are now conducting experiments and developing a simulation model to obtain the orders and rate constants of the reactions of O_3 with bacteria. The results will be reported soon [37].

Author details

Fumio Okada*
Department of Chemical Systems Engineering, University of Tokyo, Tokyo, Japan

Kazunari Naya
Research & Development Office, FRD, Inc., Toda-shi, Japan

Acknowledgement

The authors thank Prof. Y. Yamaguchi, Associate Prof. Y. Tsuji and Assistant Prof. S. Inasawa of the Department of Chemical Systems Engineering, University of Tokyo, for their kind help in the instrumental analysis and for the fruitful discussion. Measurements of the impurity concentrations in water were conducted by the analytical laboratory group in the 5th building of the School of Engineering, University of Tokyo. The content in section 4 was published in Electrochim. Acta 78, pp. 495-501, K. Naya and F. Okada, "Effects of NaCl and Na_2SO_4 cathode electrolytes on electrochemical ozone production" [18], Copyright Elsevier (2012).

8. References

[1] Rice RG and Netzer A, eds., "Handbook of Ozone Technology and Application", Ann Arbor Science (Michigan, 1982).
[2] 2004/EPRI/Global Ozone Handbook: Agriculture and Food Industries; Global Energy Partners, LLC, Lafayette, CA, 2004, 1282-2-04.
[3] Kim JB, Yousef AE, and David S (1999), J. Food Prot. 62: 1071.
[4] Kataoka Y, Miyagawa Y, Koyama S, Naya K, and Fukui K (2004), Proceeding of the 3rd Ann. Meeting of Japanese Society for Functional Water, in Japanese.
[5] Wittmann G, Horvath I, and Dombi A (2002), Ozone Science & Eng. 24: 281.
[6] Mizuno T, Tsuno H, and Yamada H (2007), Ozone Sci. & Eng. 29: 55.
[7] Stucki S, Theis G, Kotz R, Devantay H, and Christen H. J (1985), J. Electrochem. Soc. 132(2): 367.
[8] Feng J, Johnson DC, Lowery S N, and Carey J. J (1994), J. Electrochem. Soc. 141: 2708.

* Corresponding Author

[9] Santana MHP, De Faria LA, and Boodts FC (2004), Electrochim. Acta 49: 1925.
[10] Cheng SA, and Chan KY (2004), Electrochem. and Solid-State Lett. 7(3): 134.
[11] Wang YH, Cheng S, Chan KY, and Li XY(2005), J. Electrochem. Soc. 162: D197.
[12] Awad M. I, Seta S, Kaneda K, Ikematsu M, Okajima T, and Ohsaka T(2006), Electrochem. Commun. 8: 1263.
[13] Arihara K, Terashima C, and Fujishima A (2006), Electrochem. and Solid-State Lett. 9(8): D17.
[14] Kitsuka K, Kaneda K, Ikematsu M, Iseki M, Mushiake K, and Ohsaka T (2010), J. Electrochem Soc. 157: F30.
[15] Marselli B, Garcia-Gomez J, Michaud PA, Rodrigo MA., and Comninellis C (2003), J. Electrochem. Soc. 150(3): D79.
[16] Ed. by Allen J. Bard (1974) "Encyclopedia of Electrochemistry of the Elements, Vol. II, Chapter II-5: Oxygen": M. Dekker, New York.
[17] Okada F and Naya K (2009), J. Electrochem. Soc. 156: E125.
[18] Naya K and Okada F, Electrochim. Acta 78: 495.
[19] Pourbaix M (1966), "Atlas of Electrochemical Equilibria in Aqueous Solutions": Pergamon Press.
[20] Miyake N, Wakizoe M, Honda E, and Ohta T (2005), ECS Transactions 1(8): 249.
[21] Kusakabe K, Kawaguchi K, Maehara S, and Taneda M(2007), J. Chem. Eng. Japan 40(6): 523.
[22] Yamanaka I and Murayama T, Angrew. Chem(2008). Int. Ed. 47: 1900.
[23] Onda K, Ohba T, Kusunoki H, Takezawa S, Sunakawa D, and Araki T (2005), J. Electrochem. Soc. 152: D177.
[24] McBride JR, Graham GW, Peters CR, and Weber WH (1991), J. Appl. Phys. 69: 1596.
[25] Birss VI, Chang M, and Segal J(1993), J. Electroanal. Chem. 355: 181.
[26] Novak DM and Conway BE (1981), J. Chem. Soc. Faraday Trans. I, 77: 2341.
[27] Ed. by the Electrochemical Society of Japan (2000), "Denki-Kagaku Binran 5th Edition": Maruzen, in Japanese.
[28] Shibata S (1963), Bull. Chem. Soc. Japan 36: 525.
[29] Shibata S (1964), Bull. Chem. Soc. Japan 37: 410.
[30] Shibata S (1976), Electrochimica Acta 22: 175.
[31] Gottesfeld S, Yariv M, Laser D, and Srinivasan S (1977), J. Phys. Colloques 38: C5-145.
[32] Gottesfeld S, Maia G, Floriano JB, Tremiliosi-Filho G, Ticianelli EA, and Gonzalez ER (1991), J. Electrochem. Soc. 138: 3219.
[33] Tremiliosi-Filho G, Jerkiewicz G, and Conway BE (1992), Langmuir 8: 658.
[34] Jerkiewicz G, Vatankhah G, Lessard J, Soriaga MP, and Park YS (2004), Electrochimica Acta 49: 1451.
[35] Okada F, Tsuji Y, and Naya K, in preparation.
[36] Ota K, Nishigori S, and Kamiya N (1988), J. Electroanal. Chem. 257: 205.
[37] Kataoka Y, Naya K, and Okada F, in preparation.